Romanian Reports in Physics **70**, 512 (2018)

THE EFFECT OF ANNEALING ON THE STRUCTURAL AND OPTICAL PROPERTIES OF ZnSe THIN FILMS

N. TIGAU, S. CONDURACHE-BOTA

"Dunarea de Jos" University of Galati, Chemistry, Physics and Environment Department, Faculty of Sciences and Environment, Romania, 111 Domneasca Street, 800201 Galati, Romania
E-mails: *ntigau@ugal.ro; scondurache@ugal.ro*

Received December 4, 2017

Abstract. Zinc selenide (ZnSe) thin films were deposited onto glass substrates by vacuum evaporation and then were annealed at 500 K for 1h, in open atmosphere. The morpho-structural analysis of both the as-deposited and of the annealed films was performed, by using the XRD and SEM techniques. Also, by recording the transmittance and reflectance spectra, relevant optical parameters could be computed, such as the absorption coefficient, the refractive index and the optical energy bandgap. It was found that the annealing process improved the crystallinity of the films, decreased the absorption coefficient and increased the energy bandgap from 2.64 to 2.83 eV.

Key words: Zinc selenide, thin films, annealing, optical properties.

1. INTRODUCTION

Current micro- and optoelectronic devices cannot be conceived without semiconducting thin films. Their large surface-to-volume ratios and inherent specific properties given by the reduced sizes make them useful for a wide variety of applications.

Chalcogenide thin films, *i.e.* films containing at least one chalcogen element, such as S, Se or Te as major constituent were noticed and intensively prepared and studied as behaving as semiconductors in either amorphous or crystalline state, with wide, direct-type of energy bandgaps varying between 1 and 3 eV [1]. Such films exhibit high transparency over the visible spectrum and a large part of the infrared [2], recommending them for optoelectronic applications, such as infrared windows, lenses and prisms [3]. The direct bandgap of chalcogenides determines their luminescent properties, as these materials are capable of light emission upon relaxation of their electrons, previously excited by an external stimulus, such as charged particles, light (*e.g.* laser radiation) or an electric field [4]. Photoluminescent materials are intensively searched since they are mandatory for modern displays for TVs, mobile phones, light-emitting diodes, etc. [5]. Also, the large energy bandgap of the chalcogenide films makes them useful for solar cells, whose demand increases

in the context of finding more efficient renewable energy resources, in the context of finite and exhausting conventional fuels [2].

Zinc selenide is a very interesting and, therefore, studied chalcogenide, especially in the thin films forms, because it exhibits all the above-mentioned properties of chalcogenide thin films, with specific behavior and values of its relevant physical-chemical parameters, such as large energy bandgap, typically surpassing 2.65 eV [2, 7–10], with a cubic or hexagonal structure [9–13], low resistivity, high photosensitivity [8] and high optical transmittance [9, 12]. Multiple uses were found for ZnSe thin films, such as for: luminescent devices, such as light emitting diodes in the visible region [2, 8, 11, 12, 14–16], solar cells (especially since it is large energy bandgap and environmental friendly, opposite to the CdS and CdTe compounds, that were commonly used since recently) [2, 6, 17], lenses for IR lasers [2, 18], lithium ion batteries [19],

Multiple deposition methods were employed for the preparation of ZnSe thin films, since, as for any such low-dimensional structure, the type and parameters of the deposition method and also of the subsequent annealing (largely used) strongly influence the morpho-structural properties of the resulting films and inherently, strongly determine their optoelectronic properties and other physical and/or chemical features [10]. Thus, the following methods were employed: the hydrothermal method [19], the inert gas condensation method [8], metal-organic-chemical-vacuum-deposition, MOCVD [20], RF magnetron sputtering [13, 21, 22], molecular beam epitaxy [23], physical vapor deposition under vacuum, either classical or by using the quasi-closed volume technique [8–10, 12], chemical bath deposition [16], pulsed laser deposition [24], spray pyrolysis [25], electrodeposition [26] and molecular beam epitaxy [27].

Among such a long list of deposition methods for ZnSe thin films, thermal evaporation in vacuum is one of the most inexpensive and versatile, provided that high vacuum is achieved in the deposition chamber and good quality primary materials are available, such as clean and robust substrates (glass [6, 9–12, 28, 29], ITO [10], silicon [13], platinum [30] or copper [31]) and high-purity ZnSe, in either form.

We propose here the analysis of the post-deposition annealing on the structure and the optical properties of ZnSe thin films deposited by classical thermal evaporation in vacuum on glass substrates. The annealing process is commonly used for as-prepared thin films, since most often it leads to their morpho-structural stabilization and to a crystallinity improvement, by defects removal and higher crystalline grains. Especially defects and strains strongly affect the optical properties of as-deposited films, since they worsen the surface morphology and they introduce energy levels in the forbidden bandwidth, leading to a decrease of the energy bandgaps, which is a non-desirable effect, since materials with large energy bandgaps are useful in many optoelectronic applications, such as solar cells or photodiodes [10].

Both the deposition conditions and those of the annealing process were not reported by other and the results of the optical analysis proved, as compared to the literature, that ZnSe thin films with novel properties were prepared, which recommend them for many of the optoelectronic applications listed above for chalcogenide materials.

2. EXPERIMENTAL DETAILS

ZnSe thin films were deposited onto alcohol-cleaned microscope glass slides as substrates, by classical thermal evaporation in vacuum at 5×10^{-5} torr residual pressure, in a standard vacuum unit. High-purity (99.999 %) polycrystalline powder of the compound was used as source material.

The substrates were kept at room temperature during the ZnSe depositions. This choice of low temperature deposition for the films was not random. Thus, on one side, hot substrates require time and money; not only that high temperature substrates require a longer deposition time, such that the substrates could be heated, but also because as the substrates are hotter, high vacuum is reached much slower. On the other side, it was found that not only when ZnSe thin films are deposited, but also when many other types of films are to be prepared, high substrate temperatures lead to high mobility (*i.e.* enhanced diffusion) of the atoms and molecules that have to deposit, along with increased rates of their desorption from the substrates. As a consequence, at high substrate temperature, thin films tend to have poor uniformity and poor or no crystallinity at all (*i.e.* they are amorphous) [9]. Therefore, room temperature was considered a good choice for the deposition in vacuum of our ZnSe thin films, as other researchers also reported [8, 9, 28].

As explained above, annealing is generally recommended for many as-deposited thin films, leading to films stabilization and improving the crystallinity. Thus, we proceeded as such. Some of the as-deposited ZnSe films were submitted to thermal treatment, after being removed from the deposition chamber. The annealing was performed for 1 hour, in open atmosphere, the films reaching a maximum temperature of 500 K (227ºC). The thermal treatment was performed by means of a home-made device, provided with a sensitive thermocouple for temperature control. The choices of annealing conditions (*i.e.*: open air, rather low temperature of 500 K and long duration, of one hour) were not reported so far in the scientific literature. Thus, Sharma *et al.*, 2014 report the vacuum deposition of ZnSe thin films by inert gas condensation method, followed by 473 K vacuum annealing, for one hour at 473 K [8], while Öztaş *et al.*, 2005 obtained ZnSe thin films by spray pyrolysis and annealed their films up to 400ºC for 60 min in an open air furnace [32]. Also, Khan *et al.*, 2016 annealed their ZnSe films for 10 min, in the 350–500ºC temperature range, under rough vacuum conditions, for the films deposited on glass and ITO substrates, while for the ZnSe on ITO also air annealing was performed [10].

Instead, in [28], ZnSe films were annealed in an oven at 200, 300 and 400ºC, respectively.

The thickness of thin films was determined by the multiple-beam Fizeau fringe method at reflection of monochromatic light, by means of a MII-4 Linnik interferential Microscope. All samples had about 0.43 μm thickness.

The structural analysis was performed by recording the X-ray diffraction spectra of both the as-deposited and of the annealed films by using a DRON-3 diffractometer, operating at the Co-Kα line (λ = 1.7927 Å).

Scanning Electron Microscopy (SEM) was used for the morphological study of the films, whose surface aspect it is known to strongly influence the optical properties. A Philips Quanta 200 Scanning Electron Microscope was the available device, operated at 15 kV acceleration voltages. The microscope is also capable of elementary quantitative analysis by means of EDAX (Energy Dispersive X-ray Spectroscopy), with a liquid nitrogen-cooled X-ray detector.

A Perkin Elmer Lambda 35 UV-VIS-NIR double-beam Spectrometer with dual light sources was used to get the optical transmission and reflection spectra of the films, in the 300-1100 nm spectral range. Air was used as reference in the case of the transmittance measurements, while for the reflectance data, a high-quality quartz mirror was used as landmark.

The most relevant optical constants were inferred for both the as-deposited and the annealed ZnSe thin films: the absorption coefficient, α, the extinction coefficient, *k*, the refractive index, *n*, and the optical energy bandgap, E_g, as explained elsewhere [33–35].

3. RESULTS AND DISCUSSION

Figure 1 presents the XRD spectra of the ZnSe thin films under study both before and after their annealing. It was inferred that the films present a cubic (also known as zinc blende) structure, with the crystallites preferentially oriented with the (111) planes parallel to the substrates and a high texturing degree, as obtained my most researchers when preparing ZnSe films deposited not only on glass, but also on several other types of substrates [9, 11, 12, 21].

From Fig. 1 it is clear that the annealing process improves the crystallinity of the films, a proved by the increase of the intensity of the (111)-assigned XRD peak. A mild shift of this peak towards higher angular position was also noticed (*i.e.* 31.58 for the as-deposited films and 31.60 for the annealed films, respectively), which, by using the Bragg diffraction equation, leads to the conclusions that the interplanar distance, d mildly decreases with annealing from $d = 3.294$ Å to $d = 3.292$ Å (values slightly bigger than obtained by others [9], such that a more closely-packed structure is attained after annealing, behavior also observed by Khan et al., 2016 [10]).

Scherrer's formula [36] was applied to compute the mean crystallite sizes, *D*, as showed in the inset from Fig. 1. Thus, the as-deposited films have 28.55 nm average grain sizes, while the annealed films contain bigger grains, with 47.21 nm average size, values which are similar or even lower than those obtained by others [11, 12, 28]. There is a total agreement with others in which concerns the grain increase upon annealing [10, 37].

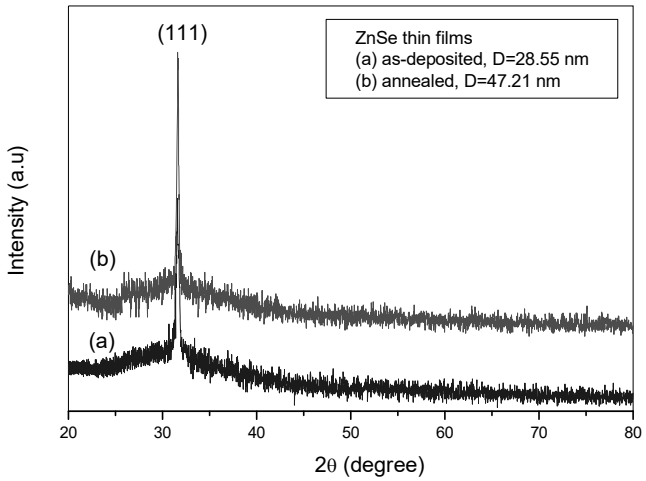

Fig. 1 – The XRD patterns of both the as-deposited and the annealed ZnSe thin films.

Figure 2 presents the SEM micrographs of the ZnSe films under study before and after annealing. From these images, the crystallinity of the films is also clear, since the grains are readily visible on the surface of the substrate. After annealing, the uniformity of the deposition improves, such as lines of grains at an even much higher magnification than for the as-deposited films can be seen to spread all over the surface. Such an aspect of the surface of ZnSe thin films was found only at [38].

As stated in [39], high quality thin films need not only single-phase and textured columnar structure, such as obtained by us, but also a stoichiometric chemical composition. Therefore, an EDAX analysis is necessary, if available. Figures 3 and 4 exhibit the EDAX spectra and the explicit qualitative and quantitative analysis as inset tables.

Both EDAX spectra from Figs. 3 and 4 present not only Zn and Se peaks, but also a silicon and an oxygen peaks, arising from the glass substrates. The stoichiometry of both the as-deposited and the annealed films is very good, with a 1.064 atomic ratio between Se and Zn for the as-deposited films, with slightly more Se than Zn, while the annealed films present a 1.084 atomic ratio between Zn and Se, this time in favor of Zn. Such a stoichiometry is equal or even better than that reported by others [12, 40–42].

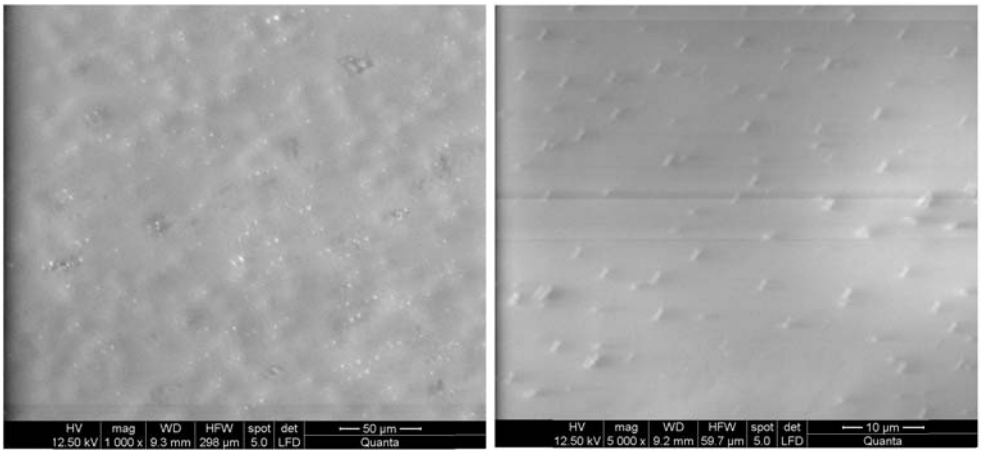

Fig. 2 – SEM micrographs of the as-deposited (on the left) and annealed (on the right) ZnSe thin films.

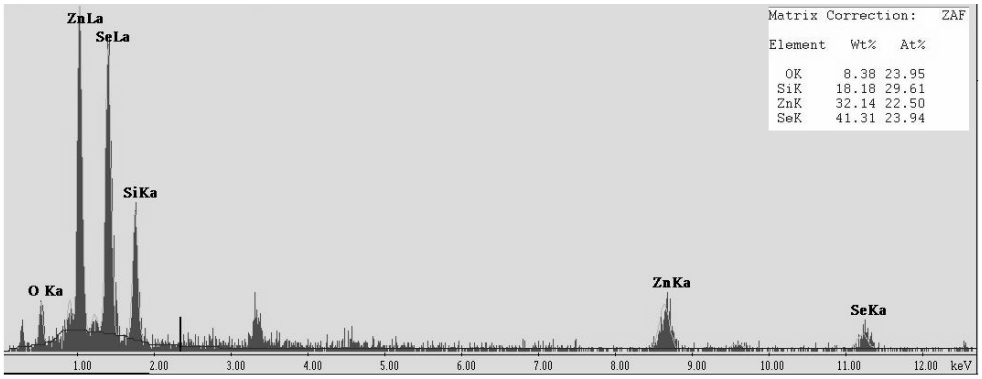

Fig. 3 – The EDAX spectrum and elementary analysis of the as-deposited ZnSe thin films.

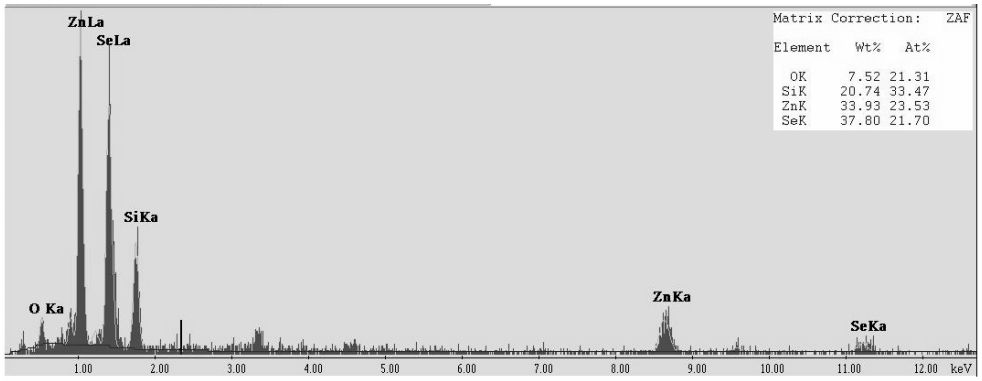

Fig. 4 – The EDAX spectrum and elementary analysis of the annealed ZnSe thin films.

Passing to the optical analysis, the transmission and reflection spectra of both the as-deposited and the annealed films are showed in Fig. 5 for the 300–1100 nm spectral range, proving, from the optical point of view, the uniformity of the depositions, which often lead to interfence-type of transmission and reflection spectra, such as the ones in Fig. 5, being due to multiple reflections at the interfaces [11]. Such spectra for ZnSe thin films were also reported by others [9, 11, 12].

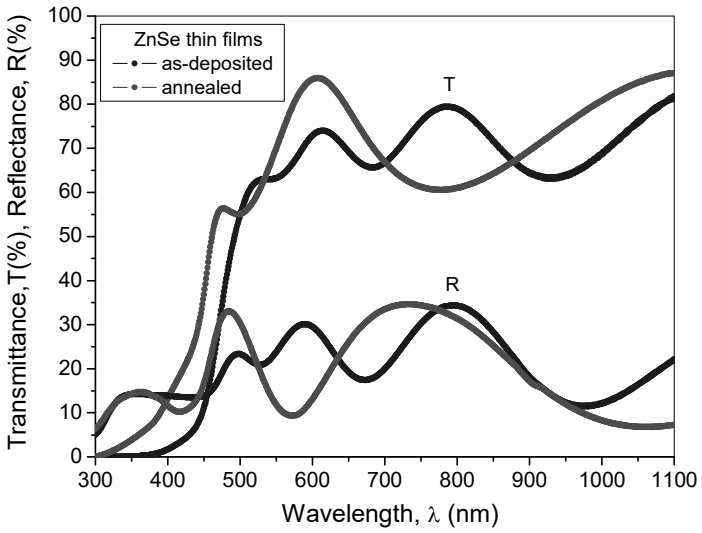

Fig. 5 – The UV-VI-NIR transmission and reflection spectra of both the as-deposited and the annealed ZnSe thin films.

There are obvious variations of both the optical transmittance and of the optical reflectance of the ZnSe films under study after annealing. In the central part of the visible range, *i.e.* between roughly 520–620 nm, the transmittance, *T* increases after annealing, while the reflectance decreases and this is also the case above 880 nm, *i.e.* in the Near-infrared. An opposite behavior is noticeable between 620–880 nm, proving that this kind of films could be used for wavelength selective optical behavior. Such wavelength-dependence of the transmittance of ZnSe films after annealing was also reported by others [8], but with lower values for *T* than for our films which exhibit along most of the visible range and the Near-infrared, the films have a very good transmittance (> 60 %), while the reflectance does not reach 40%.

By using the methods described in [33–35], the most important optical parameters of the ZnSe films under study were computed: i) the absorption coefficient, α; ii) the extinction coefficient, k; iii) the refractive index, n, and iv) the optical energy bandgap, E_g. The dependences on photon energy, ($h \cdot \upsilon$) or on wavelength, λ of the first 3 optical parameters listed before are given in Figs. 6, 7 and 8, respectively, in a comparative manner between the as-deposited and the annealed ZnSe films.

The first computed relevant optical parameter, namely the absorption coefficient has values up till $12 \cdot 10^4$ cm^{-1} over the investigated spectral range. Such values of α were also reported in [8, 12], while higher values, up till 10^7 cm^{-1} were obtained by others [43, 44].

After annealing, the absorption strongly decreases for photon energies higher than 2.5 eV, corresponding to wavelengths lower than 495 nm, *i.e.* at the end of the visible range towards UV and in the UV. The absorption is very low in most of the Visible and in the Near-infrared, recommending these films for VIS and IR windows, lenses and prisms [3].

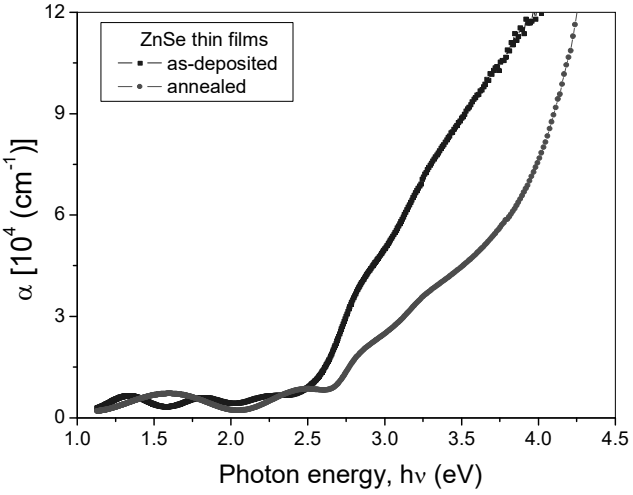

Fig. 6 – The wavelength dependence of the absorption coefficient of both the as-deposited and the annealed ZnSe thin films.

As the extinction coefficient of the ZnSe films is concerned, it was stated that it is a measure of the fraction of light lost due to scattering and absorption per unit distance of the penetration medium [12]. Its evolution with wavelength is opposite to that of the absorption coefficient as a function of photon energy, as it can be seen from Fig. 7. Still, its values are relevant for themselves, ranging between 0.01046 at 604 nm for the annealed film up till 0.35356 at 270 nm for the same film. Below 495 nm, the extinction coefficient decreases after annealing.

The decrease with increasing wavelength of the extinction coefficient of both as-deposited and of the annealed films below 495 nm was also observed in [12] and explained as the decrease of the fraction of light lost due to scattering and absorbance.

The refractive index of a material is crucial for its potential optical applications. Its variation with wavelength generally follows the trend of the reflectance spectrum of the thin film under study, as proved by Figs. 5 and 8.

The values of the refractive index of our films range between 1.75 and almost 4 at the IR-end of the visible range, values which are in good agreement with those reported by others [11, 12, 43].

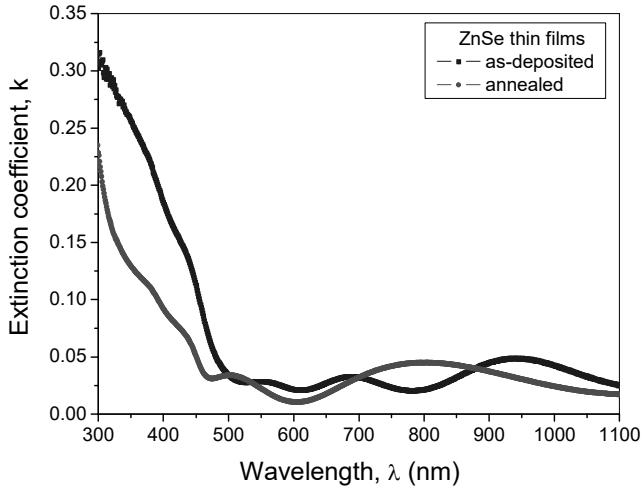

Fig. 7 – The wavelength dependence of the extinction coefficient of both the as-deposited and the annealed ZnSe thin films.

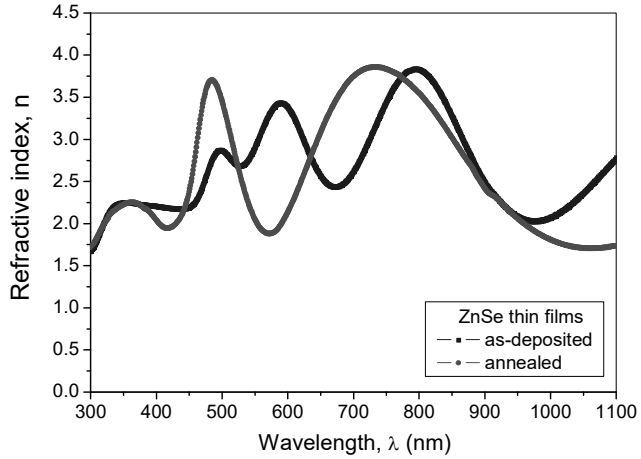

Fig. 8 – The refractive index dispersion with wavelength for both the as-deposited and the annealed ZnSe thin films.

Finally, the optical energy bandgap, E_g, of the investigated ZnSe thin films was determined from the sharply falling transmission region within the $(\alpha \cdot h \cdot \upsilon)^2$ dependence on photon energy, $(h \cdot \upsilon)$, as showed in Fig. 9, dependences corresponding to direct allowed transitions [33]. The sharp absorption edge it is considered to be

related to the stoichiometry of the films, proved by the EDAX analysis presented above [45]. The as-deposited films have a 2.64 eV energy bandgap, which increases to 2.83 eV after annealing is performed. These values are in excellent agreement with most reports in literature [2, 16, 32, 37, 46, 47].

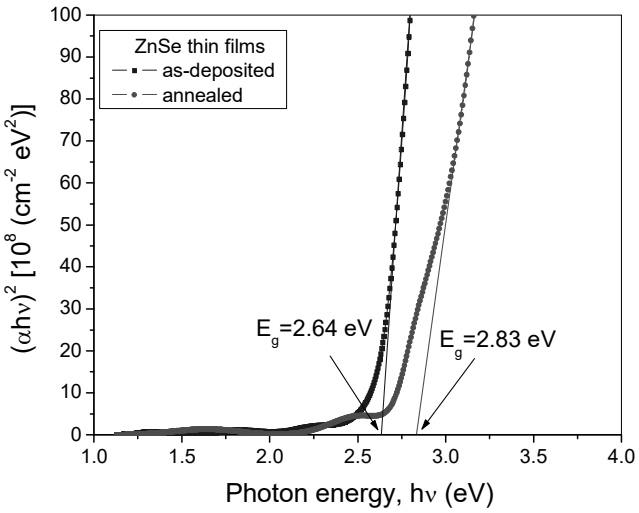

Fig. 9 – The direct-type of energy bandgap plots of $(\alpha h\nu)^2$ *versus* photon energy, (hν) for both the as-deposited and the annealed ZnSe thin films.

The increase of the energy bandgap after the thermal treatment (*i.e.* the blue shift of E_g) is most likely a consequence of structural improvement of the films, which leads to fewer defects that may introduce energy levels in the forbidden band and decrease E_g. A similar behavior is reported by [28, 48], but an opposite behavior (*i.e.* the left shift of E_g upon annealing) was also noticed by others [8, 32].

These high values for E_g in the case of our ZnSe films, corresponding to blue radiations, recommend our ZnSe thin films for blue light emitting diodes, for solar cells and for other optoelectronic applications.

4. CONCLUSIONS

This article presented the analysis of the influence of annealing on the morpho-structural and optical properties of zinc selenide thin films deposited on glass substrates by vacuum thermal evaporation. The deposition went on room temperature for the substrates. The proposed annealing lasted one hour at 500 K and in open atmosphere.

Highly textured, cubic-films were obtained, with the crystallites preferentially oriented with the (111) planes parallel to the substrates. The annealing improved

the structure of the films, leading to bigger grains and to a more uniform surface. The stoichiometry of the depositions was excellent.

The optical transmittance of the studied ZnSe films proved to be high and grew after annealing in the Near-infrared. The refractive index of the films almost reached the value of 4, with some narrow spectral regions with abnormal dispersion. The energy bandgap of the investigated ZnSe films grew from 2.64 to 2.83 eV upon annealing, as the crystallinity of the films improved.

The proposed set of deposition method, deposition condition and thermal treatment, along with the resulting properties of the zinc selenide thin films presented here recommend such films for various optoelectronic applications.

REFERENCES

1. M. Popescu, J. Non. Cryst. Solids **352**, 887–891 (2006).
2. R. K. Pathak and S. Bais, Int. J. Adv. Eng. & Technol. **7** (4), 1300–1305 (2014).
3. L. Plucinski, R. L. Johnson, A. Fleszar, W. Hanke,W.Weigand, C. Kumpf, C. Hesks, E. Umbach, T. Schallenberg and L. W. Molenkamp, Physical Review B **70**, 125308 (2004).
4. S. Kumar, P. Y. Khan, N. K.Verma and S. K. Chakarvarti, Chalcogenide Letters **5** (7), 143–152 (2008).
5. L. Strizik, T. Wagner, V. Weissova, J. Oswald, K. Palka, L. Benes, M. Krbal, R. Jambor, C. Koughia and S. O. Kasap, J. Mater. Chem. C **5**, 8489 (2017).
6. C. Natarajan, M. Sharon, C. Clement Levy and M. Spallart Newmann, Thin Solid Films **237**, 118–123 (1994).
7. V. Mittal, N. P. Sessions, J. S. Wilkinson, and G. S. Murugan, Opt. Mater. Express **7** (3), 712–725 (2017).
8. J. Sharma, D. Shikha and S.K. Tripathi, Rom. Rep. Phys. **66** (4), 1002–1011 (2014).
9. T. M. Khan, M. F, Mehmood, A. Mahmood, A. Shah, Q. Raza, A. Iqbal and U. Aziz, Thin Solid Films **519**, 5971–5977 (2011).
10. N. A. Khan, A. Saleem, A. Satti, M. Imran and A. A. Khurram, J. Mater. Sci.: Mater. Electron. **27** (9), 9755–9760 (2016).
11. M. M. Ivashchenko, I. P. Buryk, A. S.Opanasyuk, D. Nam, H. Cheong, Ja. G. Vaziev and V. V. Bibyk, Mat. Sci. Semicon. Proc. **36**, 13–19 (2015).
12. D. Prakash, E. R. Shaaban, M. Shapaan, S. H. Mohamed, A. A. Othman and K. D. Verm, Mater. Res. Bull. **80**, 120–126 (2016).
13. A. Rizzo, L. Caneve, S. Scaglione and M. A. Tagliente, Proc. SPIE Advances in Optical Interference Coatings **3738**, 40–47 (1999).
14. K. R. Murali, S. Dhanapandiyana and C. Manoharana, Chalcogenide Lett. **6** (1), 51–56 (2009).
15. S. Armstrong, P. K. Datta and R. W. Miles, Thin Solid Films **403–404**, 126–129 (2002).
16. S. Thirumavalavana, K. Manib and S. Sagadevan, Mater. Today: Proc. **3**, 2305–2314 (2016).
17. S. D. Sartale, B.R. Sankapal, M. Lux-Steiner and A. Ennaoui, Thin Solid Films **480**, 168–172 (2005).
18. N. A. Okereke, I. A. Ezenwa and A. J. Ekpunobi, J. Non-Oxide Glass. **3** (3), 105–111 (2011).
19. Y. Fu, Z. Zhang, K. Du,Y. Qu,Q. Li and X. Yang, Mater. Lett. **146,** 96–98 (2015).
20. Y. Noda, T. Ishikawa, M. Yamabe and Y. Hara, Appl. Surf. Sci., **113–114**, 28–32 (1997).
21. A. Rizzo, M. A. Tagliente, L. Caneve and S. Scaglione, Thin Solid Films, **368**, 8–14 (2000).
22. A. Karatay, H. G. Yaglioglu, A. Elmali, M. Parlak and H. Karaagac, Opt. Commun. **285** 1471 (2012).
23. T. W. Kim, M. Jung, D. V. Lee, E. Oh, S.D. Lee, H. D. Jung, M. D. Kim, J. R. Kim, H. S. Park and J.Y. Lee, Thin Solid Films **298** (1–2), 187–190 (1997).

24. Y. Shen, N. Xu, W. Hu, X. Xu, J. Sun and Z. Ying, Solid State Electron. **52,** 1833 (2008).
25. A. Bougrine, A.E. Hichou, M. Addou, J. Ebothe, A. Kachouane and M. Troyon, Mater. Chem. Phys. **80**, 438 (2003).
26. T. Mahalingum, A. Kathalingum, S. Lee, S. Moon and Y. D. Kim, J. New Mater. Electrochem. Syst. **10**, 15 (2007).
27. S. K. Chan, N. Liu, Y. Cai, N. Wang, G. K. L. Wong and I. K. Sou, J. Electron. Mater. **35** (6), 1246–1250 (2006).
28. A. D. A. Buba, Brit. J. Appl. Sci. & Technol. **14** (3), 1–7 (2016).
29. M. G. Mahesha, R. N. Meghana, Meghavarsha Padiyar, Physica B **520**, 37–42 (2017).
30. M. F. Gromboni and L. H. Mascaro, J. Electroanal. Chem. **780**, 360–366 (2016).
31. R. Kowalik, P. Zabinski and K. Fitzner, Electrochim. Acta **53,** 6184–6190 (2008).
32. M. Öztaş, M. Bedir, Ö. F. Bakkaloğlu and R. Ormanci, Acta Phys. Pol. A **107** (3), 525–533 (2005).
33. S. Condurache-Bota, G. I. Rusu, N. Tigau and L. Leontie, Cryst. Res. Technol. **45** (5), 503–511 (2010).
34. S. Condurache-Bota, N. Tigau and R. Drasovean, Journal of Science and Arts, Year 10, **2** (13), 325–330, (2010).
35. R. Swanepoel, J. Phys. E: Sci. Instrum. **16**, 1214 (1983).
36. G. I. Rusu, P. Prepelita, R. S. Rusu, N. Apetroaie, G. Oniciuc and A. Amariei, J. Optoel. Adv. Matt. **8** (3), 922–926 (2006).
37. R. Chandramohan, T. Mahalingam, J. P. Chu and P. J. Sebastian, J. New Mat. Electr. Sys. **8**, 143–148 (2005).
38. T. M. Khan and T. Bibi, Chin. Phys. B **21** (9), 097303, 1–6 (2012).
39. C. J. Panchal, A. S. Opanrsyuk, V. V. Kosyak, M. S. Desai and I. Y. Profsenko, J. Nano Electron. Phy. **3**, 274–301 (2011).
40. P. Prabukanthan and G. Harichandran, J. Electrochem. Soc. **161** (14), D736-D741 (2014).
41. H. N. Desai, J. M. Dhimmar and B. P. Modi, Int. J. Engine. Res. & Technol. **4** (05), 1132–1136 (2015).
42. B. Güzeldir, M. Sağlam and A. Ateş, J. Optoel. Adv. Matt. **14** (3-4), 224–229 (2012).
43. A. P. Pardo Gonzalez, H. G. Castro-Lora, L. D. López-Carreño, H. M. Martínez and N. J. Torres Salcedo, J. Phys. Chem. Solids **75**, 713–725 (2014).
44. S. Darafarin, R. Sahraei and A. Daneshfar, J. Alloy. Compd. **658**, 780–787 (2016).
45. G. I. Rusu, V. Ciupina, M. E. Popa, G. Prodan, G.G. Rusu and C. Baban, J. Non. Cryst. Solids **352**, 1525–1528 (2006).
46. S. Antohe, L. Ion, M. Girtan and O. Toma, Rom. Rep. Phys. **65** (3), 805-811 (2013).
47. P. C. Pingale, S. T. Mane, R. V. Suryawanshi and L. P. Deshmukh, Adv. Appl. Sci. Res. **4** (3), 177–181 (2013).
48. F. I. Ezema, A. B. C. Ekwealor and R. U. Osuji, Turk. J. Phys. **30**, 157–163 (2006).